Transcriptomic Profiling of MSI-H/dMMR Gastrointestinal Tumors to Identify Determinants of Responsiveness to Anti–PD-1 Therapy

Keigo Chida[1,2,3], Akihito Kawazoe[1], Toshihiro Suzuki[2,4], Masahito Kawazu[5], Toshihide Ueno[5], Kazumasa Takenouchi[2], Yoshiaki Nakamura[1], Yasutoshi Kuboki[1], Daisuke Kotani[1], Takashi Kojima[1], Hideaki Bando[1], Saori Mishima[1], Takeshi Kuwata[6], Naoya Sakamoto[6], Jun Watanabe[3], Hiroyuki Mano[5], Masafumi Ikeda[1], Kohei Shitara[1], Itaru Endo[3], Tetsuya Nakatsura[2], and Takayuki Yoshino[1]

ABSTRACT

Purpose: Transcriptomic profiling was performed for microsatellite instability-high (MSI-H)/mismatch repair-deficient (dMMR) gastrointestinal tumors to determine the predictors of response to PD-1 blockade.

Experimental Design: Thirty-six patients with MSI-H/dMMR gastrointestinal tumors, including gastric cancer, colorectal cancer, cholangiocarcinoma, small intestine cancer, and pancreatic cancer, being treated with PD-1 blockade were analyzed. We conducted the transcriptomic analysis of gastrointestinal tumors using RNA sequencing data, including the consensus molecular subtypes (CMS) of colorectal cancer.

Results: Gene set enrichment analysis (GSEA) demonstrated that non-responders had upregulations of epithelial–mesenchymal transition, angiogenesis, hypoxia, mTORC1, TNF-α, KRAS, Wnt/β-catenin, TGF-β, and various metabolism-related signaling pathways. Meanwhile, the IFNγ pathway was enriched in responders.

On the basis of the leading-edge analysis of GSEA, *VEGF-A* was significantly correlated with enriched pathways in non-responders. Patients with high *VEGF-A* expression, compared with those with low expression, had significantly shorter progression-free survival [PFS; median 4.8 months vs. not reached (NR), $P = 0.032$] and overall survival (median 11.1 months vs. NR, $P = 0.045$). Among 13 patients with colorectal cancer evaluable for CMS classification, the objective response rate was 100%, 0%, 0%, and 16.7% in CMS1, CMS2, CMS3, and CMS4, respectively. Patients with CMS1 had significantly longer PFS (NR vs. 4.8 months, $P = 0.017$) than those with CMS2, CMS3, or CMS4.

Conclusions: Several transcriptomic features, including CMS classification and related genes, were associated with response to PD-1 blockade in MSI-H/dMMR gastrointestinal tumors. These findings can help develop predictive biomarkers or combination immunotherapies.

Introduction

Microsatellite instability-high (MSI-H) or mismatch repair-deficient (dMMR) tumors exhibit elevated mutation rates (including frameshifts or missense mutations) and hypermethylation (including hypermethylation at the *MLH1* promoter), resulting in the enhanced expression of neoantigens and high infiltration of CD8^{+} T cells into the tumor microenvironment (TME; refs. 1, 2). Tumors with these distinct molecular and immunological characteristics may respond well to immune checkpoint inhibitors (ICI; ref. 3). In several trials, the FDA has approved anti–PD-1 antibodies (e.g., pembrolizumab and dostarlimab) for patients with treatment-resistant MSI-H/dMMR solid tumors (4, 5). Currently, MSI-H/dMMR is one of the most consistent predictive biomarkers for ICIs. However, approximately 30% of MSI-H/dMMR tumors had during the first months of therapy progressive disease with anti–PD-1 therapy, and thus it is crucial to identify the predictive biomarkers or molecular profiling correlated with resistance to these agents (6–8). In our recent study of 45 MSI-H/dMMR gastrointestinal tumors, we found that tumor mutational burden (TMB)-low tumors and *PTEN* mutations, especially in the phosphatase domain with immunosuppressive microenvironments, might be associated with decreased responsiveness to PD-1 blockade (9). Other gene alterations, such as *STK11*, *FBXW7*, *JAK1*, *B2M*, and *HLA* mutations, were also observed in non-responders (9).

Aside from mutational status, gene signatures detected via RNA sequencing, especially those induced by IFNγ, may also be potential biomarkers for predicting clinical benefit to anti–PD-1 or anti–PD-L1 therapies in microsatellite-stable (MSS)/MMR-proficient (pMMR) solid tumors (10). A preclinical study reported that the Wnt/β-catenin pathway induced intrinsic resistance to ICIs in melanoma (11). However, there is a paucity of information regarding the transcriptomic landscape in MSI-H/dMMR gastrointestinal tumors treated with anti–PD-1 therapy (12). Thus, uncovering the molecular determinants of responsiveness to ICI therapy can lead to the development of novel biomarkers or combination therapeutic modalities to overcome resistance to these agents in MSI-H/dMMR gastrointestinal tumors.

This study aimed to elucidate predictors of responsiveness to ICI therapy in MSI-H/dMMR gastrointestinal tumors. We performed

[1]National Cancer Center Hospital East, Kashiwa, Chiba, Japan. [2]Division of Cancer Immunotherapy, Exploratory Oncology Research and Clinical Trial Center, National Cancer Center, Kashiwa, Japan. [3]Department of Gastroenterological Surgery, Yokohama City University Graduate School of Medicine, Yokohama, Japan. [4]General Medicinal Education and Research Center, Teikyo University, Tokyo, Japan. [5]Division of Cellular Signaling, National Cancer Center Research Institute, Tokyo, Japan. [6]Department of Pathology and Clinical Laboratories, National Cancer Center Hospital East, Kashiwa, Japan.

Translational Relevance

Approximately half of microsatellite instability-high (MSI-H)/ mismatch repair-deficient (dMMR) tumors do not respond to immune checkpoint inhibitors (ICI), highlighting the importance of identifying predictive biomarkers or molecular profiling correlated with resistance to these agents. We performed transcriptomic profiling of MSI-H/dMMR gastrointestinal tumors treated with PD-1 blockade, including the consensus molecular subtypes (CMS) of colorectal cancer. Our study revealed that non-responders had the enrichment of epithelial–mesenchymal transition, angiogenesis, hypoxia, mTORC1, KRAS, Wnt/β-catenin, TGFβ, and various metabolism-related signaling pathways, which have been associated with an immunosuppressive tumor microenvironment. Meanwhile, the IFNγ pathway was upregulated in responders. High expression of *VEGF-A* might predict a negative response to ICIs in this population. Moreover, CMS classification possibly correlated with clinical outcomes of PD-1 blockade in MSI-H/ dMMR patients with colorectal cancer. These transcriptomic features could help in the development of predictive biomarkers or combination immunotherapies in the future.

transcriptomic profiling of MSI-H/dMMR gastrointestinal tumors treated with PD-1 blockade, including the consensus molecular subtypes (CMS) of colorectal cancer.

Materials and Methods

Patients

We performed transcriptomic analysis to uncover the signatures associated with the PD-1 blockade response in patients with advanced MSI-H/dMMR gastrointestinal tumors at National Cancer Center Hospital East (Kashiwa, Chiba, Japan). The inclusion criteria were as follows: (i) an Eastern Cooperative Oncology Group performance status (ECOG PS) of 0 to 1; (ii) histologically proven, unresectable, locally advanced, or metastatic gastrointestinal tumor that is refractory or intolerant to at least 1 chemotherapy regimen; (iii) MSI-H or dMMR status verified via local PCR or IHC as described below; (iv) adequate bone marrow, hepatic, and renal function as indicated by medical records; (v) received an anti–PD-1 inhibitor either alone (i.e., pembrolizumab or nivolumab) or as combination therapy (i.e., pembrolizumab plus napabucasin; ref. 13) from July 2015 to April 2021; and (vi) had adequate tumor samples for RNA sequencing. All patients provided written informed consent for the biomarker analysis of formalin-fixed paraffin-embedded (FFPE) tissue specimens from archival tissue samples. The study was approved by the Institutional Review Board of the National Cancer Center Hospital East (Kashiwa, Chiba, Japan) and was carried out in accordance with the guidelines for biomedical research specified in the Declaration of Helsinki.

MSI and MMR status

MSI status was analyzed using a Promega MSI analysis system (Promega), which used 5 mononucleotide markers for the detection of MSI: BAT-25, BAT-26, NR-21, NR-24, and MONO-27 (14). Tumors were classified as MSI-H if instability was noted in at least two markers. On the other hand, MMR status was assessed via IHC using the following monoclonal antibodies: anti-mutL homolog 1 (MLH1, ES05), anti-mutS homolog 2 (MSH2, FE11), anti-postmeiotic segregation increased 2 (PMS2, EP51), and anti-mutS homolog 6 (MSH6,

EP49; Agilent Technologies). Tumors that lacked MLH1, MSH2, PMS2, or MSH6 expression were considered dMMR.

Whole-exome sequencing

Mutational status, including TMB, was assessed via whole-exome sequencing as we previously reported (9). TMB was defined as the total number of nonsynonymous mutations, including indels, mutations per megabase (muts/Mb) in whole-exome sequencing and TMB-high was defined as ≥ 10 muts/Mb.

RNA sequencing

Total RNA was extracted from FFPE specimens using the RNeasy FFPE Kit (QIAGEN). Ribosomal RNA was depleted from the total RNA with an NEBNext rRNA Depletion Kit (New England Biolabs). Sequencing libraries for RNA-seq were prepared with a NEBNext Ultra RNA Library Prep Kit (New England Biolabs); these prepared RNA-seq libraries underwent 150 bp, paired-end NGS sequencing. To perform a gene set enrichment analysis (GSEA), the gene set variation analysis (GSVA) in R package and the GSEA tool (https://www.gsea-msigdb.org/gsea/index.jsp) were used to calculate the signaling pathway variation score and normalized enrichment score (NES), respectively (15, 16). In GSEA, gene sets with both nominal P value and FDR q value of <0.05 were considered as significantly enriched pathways. These analyses were performed according to the hallmark gene sets, which were downloaded from the Molecular Signatures Database (MSigDB). After GSEA, leading-edge analysis was performed to determine genes with a high impact on each pathway; the genes that overlapped across significant pathways were further identified (15, 16). A unique CMS in patients with colorectal cancer was also assessed as previously described (17).

Multiplex immunofluorescence IHC and PD-L1 expression

The protein expression levels of CD3, CD4, CD8, and cytokeratin in FFPE samples were assessed using multiplex fluorescence IHC with each monoclonal antibody. The details of multiplex immunofluorescence are available in the Supplementary Methods.

A trained pathologist (T. Kuwata) who was blinded to the diagnoses and/or other identifying information assessed the PD-L1 combined positive score (CPS) using PD-L1 IHC 22C3 pharmDx (Dako). CPS was defined as the ratio of the number of PD-L1–positive cells (including tumor cells, lymphocytes, and macrophages) to the total number of tumor cells multiplied by 100.

Outcomes and statistical analysis

Progression-free survival (PFS) was defined as the time from the initiation of PD-1 blockade to disease progression or death from any cause. Overall survival (OS) was defined as the time from the initiation of PD-1 blockade to death from any cause. Tumor response was assessed in patients with measurable lesions using the RECIST version 1.1. Overall response rate (ORR) was defined as the proportion of patients whose best overall response was a complete response (CR) or partial response (PR). Disease control rate (DCR) was defined as the proportion of patients who achieved a best overall response of a CR, PR, or stable disease (SD) lasting more than 6 weeks from the start of study treatment.

Quantitative data are expressed as median and interquartile range (IQR) and the cutoff values were set to the median. The Wilcoxon rank sum test was used to compare continuous variables, whereas Fisher's exact test was used to compare categorical variables. Survival curves were estimated using the Kaplan–Meier method, and differences between groups were tested using the log-rank test. Hazard ratios

(HR) were estimated using the Cox proportional hazards model. PFS and OS were analyzed using univariate and multivariate Cox regression analyses. The backward selection method was used to select factors retained in the multivariate analysis ($P < 0.1$). All P values of <0.05 were considered statistically significant. All statistical analyses were performed using the statistical program R version 4.1.0 (The R Foundation for Statistical Computing).

Data availability

Raw RNA sequencing data used in the present study were uploaded to the Sequence Read Archive of DNA DataBank of Japan (DRA: https://www.ddbj.nig.ac.jp/dra/index.html) under accession No. DRA013565. All other data are available from the corresponding author upon reasonable request. Those requests will be reviewed by a study steering committee to verify whether the request is subject to any intellectual property or confidentiality obligations.

Results

Patient overview

To examine transcriptomic profiling associated with the response to PD-1 blockade, we identified patients with gastrointestinal tumors and evaluated their characteristics and responses to PD-1 blockade. A total of 36 patients with available RNA sequencing data met the inclusion criteria and had the following cancers: gastric cancer ($n = 18$), colorectal cancer ($n = 13$), cholangiocarcinoma ($n = 2$), small intestine cancer ($n = 2$), and pancreatic cancer ($n = 1$). The patient characteristics are summarized in **Table 1**. In addition, the details of MSI/MMR status with TMB are summarized in Supplementary Table S1. Of the total 36 patients, 9 were analyzed by both Promega MSI analysis and MMR IHC test, and the remaining 27 were analyzed by either test [Promega MSI analysis ($n = 15$) or MMR IHC ($n = 12$); Supplementary Table S1]. Tumor specimens were collected from primary tumor samples before PD-1 blockade.

The maximum percentage change in tumor size from baseline is shown in **Fig. 1**. All patients had measurable lesions. The overall population had an ORR and DCR of 52.7% (19/36) and 83.3% (30/36), respectively. The median follow-up at the time of the analysis was 28.2 months. In the overall population, the median PFS was 24.5 months [95% confidence interval (CI), 4.4 to not reached (NR)], whereas the median OS was 29.5 months (95% CI, 15.2–NR), with 16 mortalities (44.4%; Supplementary Fig. S1).

Transcriptome features associated with the response to PD-1 blockade

The gene set activity in enriched pathways is illustrated using a heat map among samples calculated using GSVA, with a bar plot representing NES between non-responders [SD or progressive disease (PD)] and responders (CR or PR) generated using GSEA (**Fig. 1**). On GSEA, non-responders had upregulations of epithelial–mesenchymal transition (EMT), angiogenesis, hypoxia, mTORC1, TNFα, KRAS, Wnt/β-catenin, TGFβ, and various metabolism-related signaling pathways. On the other hand, the IFNγ and α pathways were upregulated in responders.

Next, we performed leading-edge analysis of the GSEA to identify the individual genes that were significantly related to enriched pathways in non-responders. Specifically, the top 5 genes were *VEGF-A*, *LDHA*, *ALDOA*, *IDH1*, and *PLAUR* (**Fig. 2**). Of these, patients with high *VEGF-A* mRNA expression, compared with those with low expression, had significantly shorter PFS (median, 4.8 months; 95% CI, 3.0–30.7 vs. NR, 95% CI, 8.4–NR; HR, 2.79; 95% CI, 1.10–7.09;

Table 1. Patient characteristics.

	Total ($n = 36$)
Age, y	
Median (range)	67 (30–84)
≥65	20 (55.6)
Sex, n (%)	
Male	20 (55.6)
Female	16 (44.4)
Previous treatment regimens, n (%)	
1	19 (52.8)
≥2	17 (47.2)
Primary cancer, n (%)	
Gastric	18 (50.0)
Colorectal	13 (36.1)
Small intestine	2 (5.6)
Cholangiocarcinoma	2 (5.6)
Pancreatic	1 (2.8)
ECOG PS, n (%)	
0	23 (63.9)
1	13 (36.1)
Surgery on primary tumor, n (%)	
No	14 (38.9)
Yes	22 (61.1)
Metastatic sites, n (%)	
Liver	5 (13.9)
Lung	5 (13.9)
Peritoneal	16 (44.4)
Lymph node	29 (80.6)
Number of metastatic organs, n (%)	
1	19 (52.8)
≥2	17 (47.2)
PD-L1 CPS, n (%)	
CPS < 1	7 (19.4)
1 ≤ CPS < 10	5 (13.9)
CPS ≥ 10	23 (63.9)
Missing	1 (5.3)
TMB, mutations/Mb (range)	38.7 (3.6–93.0)
Treatment, n (%)	
Nivolumab	6 (16.7)
Pembrolizumab	24 (66.7)
Pembrolizumab with napabucasin	6 (16.7)

Abbreviations: CPS, combined positive score; ECOG, Eastern Cooperative Oncology Group; PS, Performance status; TMB, tumor mutational burden.

$P = 0.032$) and OS (median, 11.1 months; 95% CI, 5.3–NR vs. NR, 95% CI, 15.2–NR; HR, 2.97; 95% CI, 1.02–8.62; $P = 0.045$; **Fig. 3**). On the other hand, the expression of the other genes was not associated with PFS and OS (data not shown). Multivariate analyses showed that high expression of VEGF-A mRNA was independently associated with shorter PFS (HR, 3.23; 95% CI, 1.18–8.87; $P = 0.023$) and OS (HR, 3.61; 95% CI, 1.06–12.29; $P = 0.040$; Supplementary Tables S2 and S3). Among other *VEGF*-related genes, the expression of *PIGF* and *PDGF-A* were significantly higher in non-responders than in responders. Furthermore, the expression of *VEGFR-1* and *PDGF-B* tended to be higher in non-responders than in responders (Supplementary Fig. S2).

CMS classification of colorectal cancer and response to PD-1 blockade

Among 13 patients with colorectal cancer evaluable for CMS classification, CMS1, CMS2, CMS3, and CMS4 were detected in 4, 2, 1, and 6 cases, respectively. Among the 4 cases of CMS1, 1 had CR,
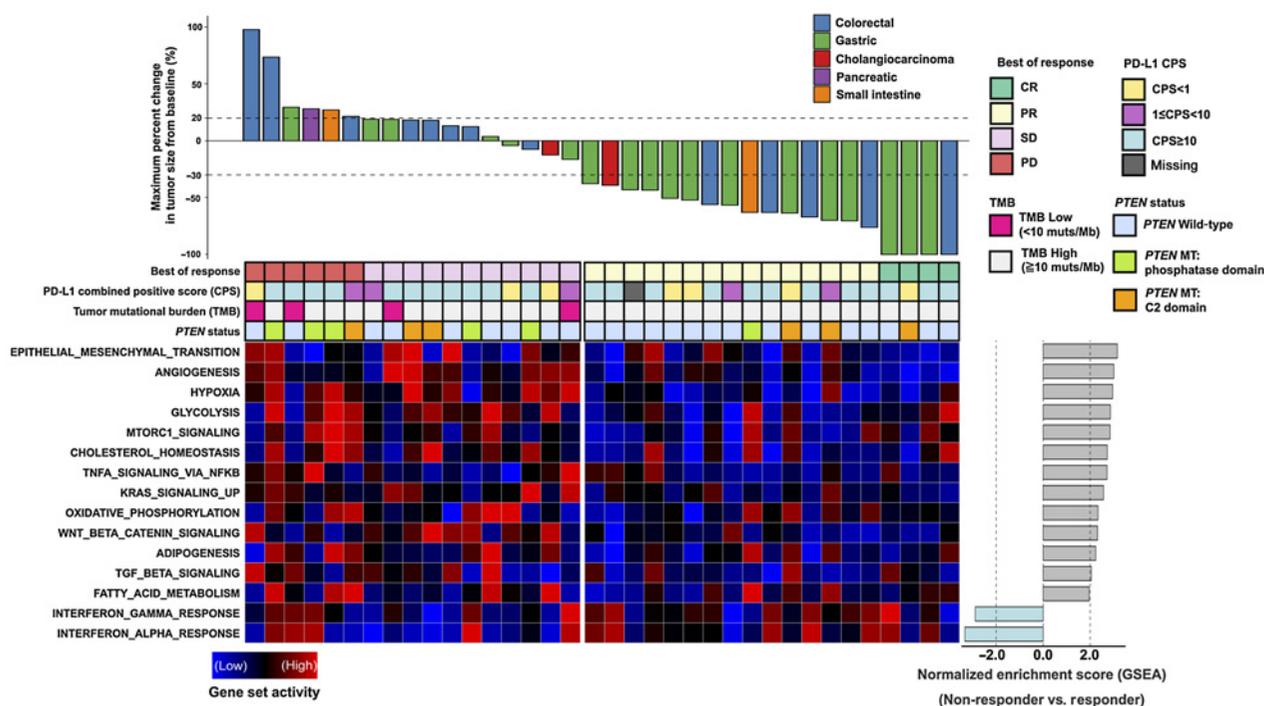
Figure 1.
Waterfall plot of the maximum percentage change in tumor size from baseline measured using the RECIST version 1.1 and gene set activity of signaling pathways between responders and non-responders. Top, percentages of maximum tumor volume changes during PD-1 blockade measured using the RECIST 1.1 criteria. The bottom dotted line represents a tumor reduction of 30%, as per RECIST 1.1, representing partial response (PR) or complete response (CR). The top dotted line represents a tumor increase of more than 20%, representing disease progression (PD). Middle, summary of best of response, combined positive score (CPS), tumor mutational burden (TMB), and *PTEN* mutation status. Each column represents an individual patient with available data. Bottom left, a heat map showing the relative expression levels of associated gene sets between samples calculated using the gene set variation analysis (GSVA). Bottom right, a bar plot representing normalized enrichment score between responders and non-responders for each gene set calculated using the gene set enrichment analysis (GSEA).

while the remaining 3 had PR. Both cases of CMS2 had SD. The single case of CMS3 had PD. Among the 6 cases of CMS4, 1 had PR, 3 had SD, and the remaining 2 patients had PD. Consequently, the ORR was 100% (4/4), 0% (0/2), 0% (0/1), and 16.7% (1/6) for CMS1, CMS2, CMS3, and CMS4, respectively (**Fig. 4**). Patients with CMS1 had a significantly longer PFS (median, NR; 95% CI, NR–NR vs. 4.8 months; 95% CI, 1.1–30.7; $P = 0.017$) and numerically longer OS (median, NR;

95% CI, NR–NR vs. 31.0 months; 95% CI, 2.6–NR; $P = 0.105$) than those with CMS2, CMS3, or CMS4 (**Fig. 5**).

TME according to the expression of *VEGF-A* mRNA

The TME was analyzed via multiplex fluorescence IHC (data shown as median; IQR). Tumors with high *VEGF-A* mRNA expression, compared with those with low expression, had significantly lower
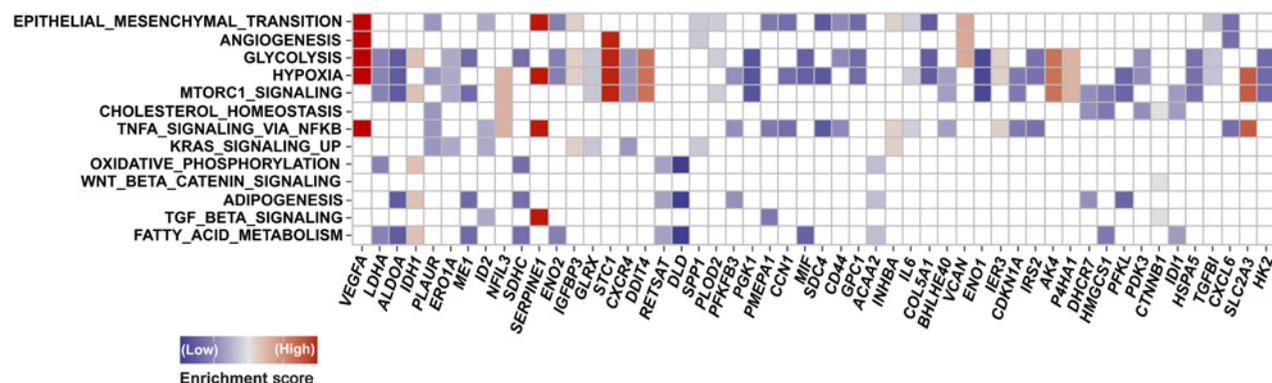
Figure 2.
The leading-edge analysis of the gene set enrichment analysis (GSEA). The heatmap created by the leading-edge analysis of the GSEA indicates the relative expression level of each gene associated with 3 or more pathways. The top 5 genes related to significantly enriched pathways in non-responders to PD-1 blockade were *VEGF-A*, *LDHA*, *ALDOA*, *IDH1*, and *PLAUR*.
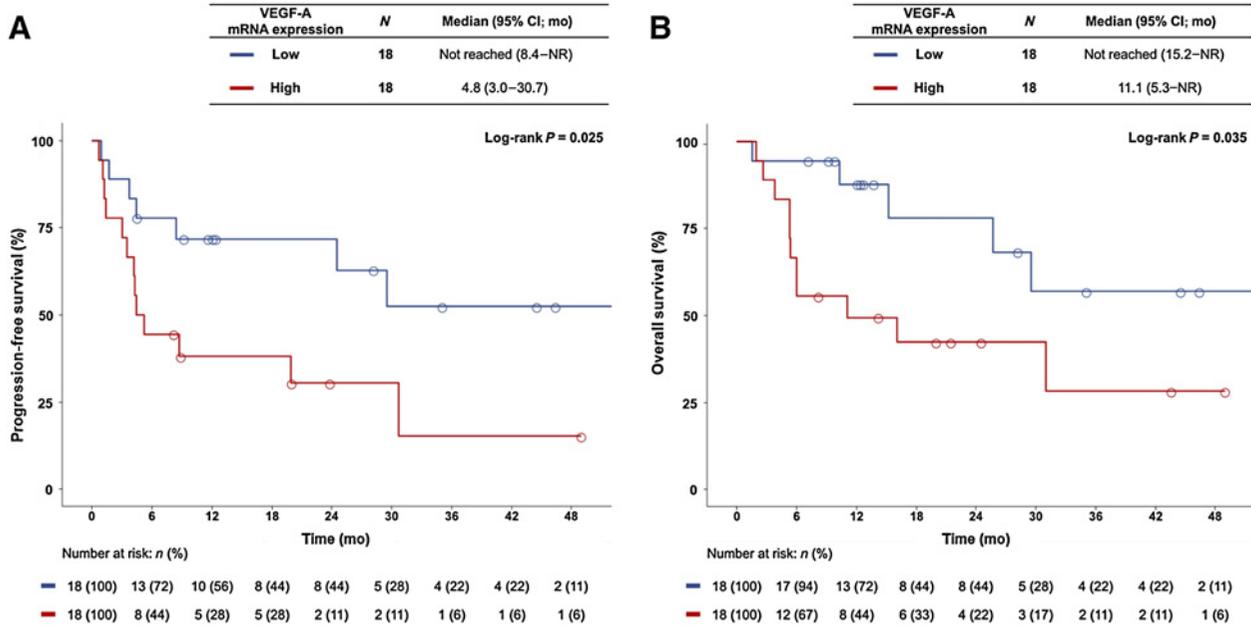
Figure 3.
Kaplan–Meier plots of progression-free survival (PFS; **A**) and overall survival (OS; **B**) according to the expression of *VEGF-A* mRNA. Patients with high *VEGF-A* mRNA expression, compared with those with low expression, had significantly lower PFS [median: 4.8 months; (95% CI, 3.0–30.7) vs. not reached, NR (95% CI, 8.4–NR); log-rank *P* = 0.025] and OS [median, 11.1 months; (95% CI, 5.3–NR) vs. NR (95% CI, 15.2–NR); log-rank *P* = 0.035].

levels of intratumoral CD8$^+$ T cells [146.8/mm^2 (95% CI, 63.7–336.2) vs. 269.1/mm^2 (95% CI, 193.1–621.2); *P* = 0.041], as well as numerically lower levels of intratumoral CD3$^+$ [352.6/mm^2 (95% CI, 258.8–471.8) vs. 414.7/mm^2 (95% CI, 348.9–873.4); *P* = 0.133] and CD4$^+$ T cells [52.1/mm^2 (95% CI, 27.1–100.1) vs. 96.1/mm^2 (95% CI, 16.3–169.2); *P* = 0.405; Supplementary Fig. S3].

Discussion

We performed transcriptomic profiling, including CMS of colorectal cancer, for patients with MSI-H/dMMR gastrointestinal tumors treated with PD-1 blockade to elucidate the determinants of respon-

siveness to ICI therapy. To the best of our knowledge, this is the first report to comprehensively describe the transcriptomic landscape of tumors (specifically related to PD-1 blockade) among patients with MSI-H/dMMR gastrointestinal tumors.

First, our study revealed that non-responders exhibited enrichment of the EMT, angiogenesis, hypoxia, mTORC1, KRAS, Wnt/β-catenin, TGF-β, and various metabolism-related signaling pathways, all of which have been associated with an immunosuppressive TME (11, 18–25). On the other hand, the IFNγ pathway was upregulated in responders, which was in line with previous studies showing that an IFNγ-related mRNA profile correlated with favorable clinical outcomes with ICIs in several malignancies (26).
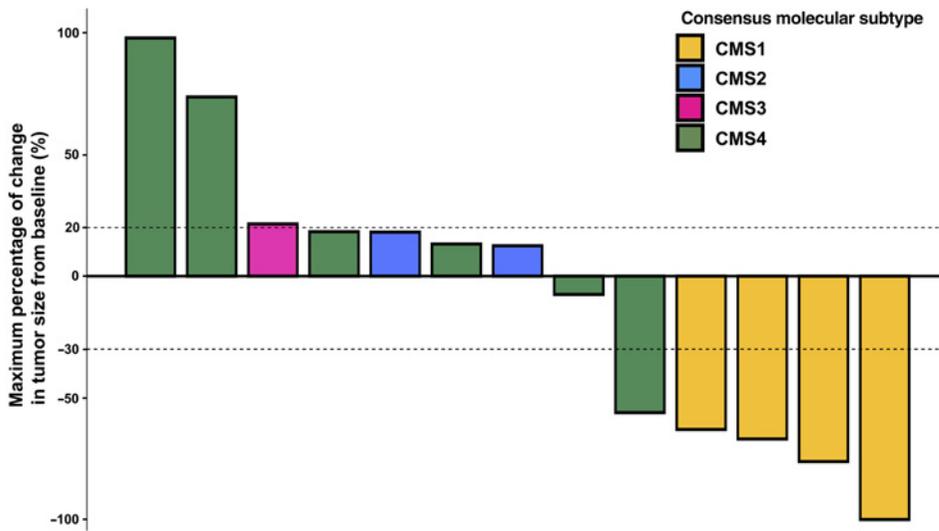
Figure 4.
Waterfall plot of the maximum percentage change in tumor size from baseline according to the consensus molecular subtype (CMS) of colorectal cancer (CRC) as measured using the RECIST version 1.1. Among 13 patients with CRC evaluable for CMS classification, CMS1, CMS2, CMS3, and CMS4 were detected in 4, 2, 1, and 6 cases, respectively. The ORR was 100% (4/4), 0% (0/2), 0% (0/1), and 16.7% (1/6) for patients with CMS1, CMS2, CMS3, and CMS4, respectively.
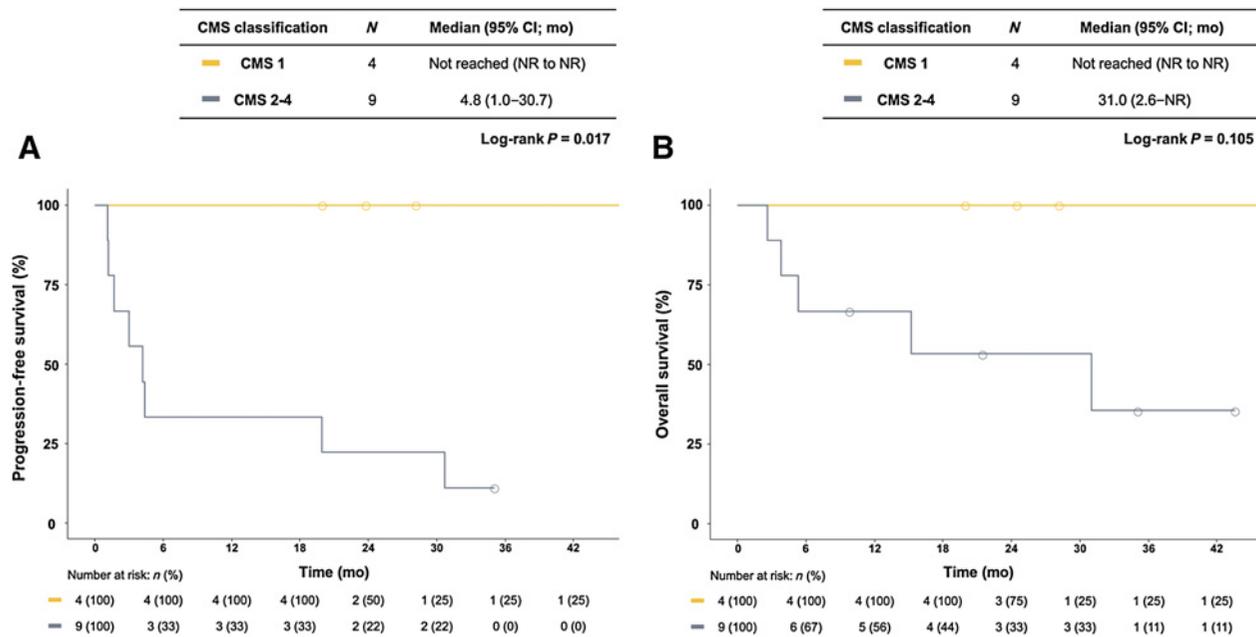
CMS classification	N	Median (95% CI; mo)
CMS 1	4	Not reached (NR to NR)
CMS 2-4	9	4.8 (1.0–30.7)
		Log-rank P = 0.017

CMS classification	N	Median (95% CI; mo)
CMS 1	4	Not reached (NR to NR)
CMS 2-4	9	31.0 (2.6–NR)
		Log-rank P = 0.105

Figure 5.
Kaplan–Meier plots of progression-free survival (PFS; **A**) and overall survival (OS; **B**) according to the expression of consensus molecular subtype (CMS). Patients with CMS1 showed significantly longer PFS [Not reached, NR (95% CI, NR–NR) vs. 4.8 months (95% CI, 1.1–30.7); $P = 0.017$] and numerically longer OS [Not reached (95% CI, NR–NR) vs. 31.0 months (95% CI, 2.6–NR); $P = 0.105$] than those with other types of CMS.

In a recent study, Kwon and colleagues (12) reported that non-responders had upregulations in the Wnt/β-catenin pathway in a phase II trial of pembrolizumab in cases of advanced MSI-H gastric cancer. Similarly, the non-responders to anti–PD-1 therapy in our cohort also demonstrated an enriched Wnt/β-catenin pathway. Recently, a selective inhibitor of the interaction between β-catenin and CREB-binding protein demonstrated synergistic antitumor activity in combination with PD-1 blockade via modulation of the Wnt/β-catenin pathway and alteration of the tumor immune microenvironments *in vivo* (27, 28). Thus, ICI resistance in MSI-H/dMMR gastrointestinal tumors can potentially be overcome by targeting the Wnt/β-catenin pathway.

In our study, non-responders to PD-1 blockade had upregulations in the pathways of angiogenesis. Moreover, on the basis of the leading-edge analysis of GSEA, tumors with high *VEGF-A* expression were associated with poorer clinical outcomes after PD-1 blockade therapy compared with those with low *VEGF-A* expression. These results were consistent with previous reports demonstrating that *VEGF-A* levels were elevated among non-responders to ICI therapy in melanoma and other cancers (29, 30). *VEGF* has been reported to reduce the infiltration of CD8$^+$ T cells through decreasing the expression of vascular cell adhesion molecule-1 and increasing the expression of Fas ligand (31, 32). In line with this, we observed significantly fewer CD8$^+$ T cells in tumors with high *VEGF-A* expression in our study. Recently, a phase III trial of atezolizumab (anti–PD-L1 antibody) plus bevacizumab (anti–VEGF-A antibody) showed promising results for hepatocellular carcinoma, leading to its FDA approval (33). Furthermore, on the basis of the results of phase III trials, the FDA has approved anti–PD-1/PD-L1 antibodies plus tyrosine kinase inhibitors of VEGF receptor in renal cell carcinoma or endometrial carcinoma (34, 35). Given that the levels of *VEGF-A* and other *VEGF* related genes (i.e., *PIGF*, *PDGF-A/ B*, and *VEGFR-1*) increased in non-responders in our

cohort, therapy with anti-*VEGF* antibodies or tyrosine kinase inhibitors of *VEGF* receptor might overcome resistance to ICIs in MSI-H/dMMR gastrointestinal tumors.

In addition, we evaluated CMS and their clinical outcomes in MSI-H/dMMR colorectal cancer. As expected, patients with CMS1, characterized by inflamed tumors with infiltrating activated lymphocytes and high levels of immune checkpoint molecules (36), exhibited a greater tumor response (ORR, 100%) and longer survival outcomes compared with the other types of CMS. Notably, among 6 patients with CMS4, only 1 patient showed an objective response, whereas 2 showed apparent tumor enlargement. CMS4 is characterized by immune-excluded tumors, wherein the immune system is engaged, but factors in its microenvironment (e.g., angiogenesis or TGFβ) prevent activity (37, 38). Thus, dual inhibition of PD-1 and angiogenesis or TGFβ might be a promising strategy for MSI-H/dMMR colorectal cancer with CMS4, warranting further investigations in future clinical trials.

The major limitations of this study were its small sample size and retrospective, single-center design. Therefore, this was a hypothesis-generating study. Further preclinical studies and larger cohort studies are needed to confirm our findings. However, given that MSI-H/dMMR is a rare subtype in patients with gastrointestinal tumors (39), our study provides new insight regarding the development of predictive biomarkers or combination therapies for PD-1/PD-L1 blockade in this population. Also, this research included different gastrointestinal cancer type even if they all shared MSI/dMMR status. The difference of primary tumor location was possibly related with that of RNA expression level (40). We should analyze transcriptomic profiling of each cancer type in a future study with a large cohort of patients, though the RNA expressions of VEGF related gene, which were significantly enriched in non-responders compared with responders, were not significantly different between primary tumor locations in

our cohort (data not shown). Finally, the proportion of CMS1 in our study was lower than in a previous report probably due to its small sample size (36). Furthermore, although Marisa and colleagues (41) recently reported that several CMS may coexist within a same colorectal cancer, the heterogeneity was not assessed in our study, which should be investigated in future studies.

In conclusion, several signaling pathways were associated with the response to PD-1 therapies in patients with MSI-H/dMMR gastrointestinal tumors. Of note, high *VEGF-A* expression might be a predictor of negative response to these agents in this population. Moreover, CMS classification possibly correlated with the clinical outcomes of PD-1 blockade in MSI-H/dMMR patients with colorectal cancer. These transcriptomic features could help in the future development of predictive biomarkers or combination immunotherapies.

Authors' Disclosures

Authors' Contributions

Acknowledgments

References

1. Chalmers ZR, Connelly CF, Fabrizio D, Gay L, Ali SM, Ennis R, et al. Analysis of 100,000 human cancer genomes reveals the landscape of tumor mutational burden. Genome Med 2017;9:34.
2. Li K, Luo H, Huang L, Luo H, Zhu X. Microsatellite instability: a review of what the oncologist should know. Cancer Cell Int 2020;20:16.
3. Chao J, Fuchs CS, Shitara K, Tabernero J, Muro K, Cutsem EV, et al. Assessment of pembrolizumab therapy for the treatment of microsatellite instability–high gastric or gastroesophageal junction cancer among patients in the KEYNOTE-059, KEYNOTE-061, and KEYNOTE-062 clinical trials. JAMA Oncol 2021;7:895–902.
4. Casak SJ, Marcus L, Fashoyin-Aje L, Mushti SL, Cheng J, Shen YL, et al. FDA approval summary: pembrolizumab for the first-line treatment of patients with MSI-H/dMMR advanced unresectable or metastatic colorectal carcinoma. Clin Cancer Res 2021;27:4680–4.
5. Markham A. Dostarlimab: first approval. Drugs. 2021;81:1213–9.
6. Marabelle A, Le DT, Ascierto PA, Giacomo AMD, Jesus-Acosta AD, Delord J-P, et al. Efficacy of pembrolizumab in patients with noncolorectal high microsatellite instability/mismatch repair–deficient cancer: results from the phase II KEYNOTE-158 study. J Clin Oncol 2020;38:1–10.
7. Le DT, Kim TW, Cutsem EV, Geva R, Jäger D, Hara H, et al. Phase II open-label study of pembrolizumab in treatment-refractory, microsatellite instability-high/mismatch repair-deficient metastatic colorectal cancer: KEYNOTE-164. J Clin Oncol 2019;38:11–9.
8. André T, Shiu K-K, Kim TW, Jensen BV, Jensen LH, Punt C, et al. Pembrolizumab in microsatellite-instability–high advanced colorectal cancer. New Engl J Med 2020;383:2207–18.
9. Chida K, Kawazoe A, Kawazu M, Suzuki T, Nakamura Y, Nakatsura T, et al. A low tumor mutational burden and PTEN mutations are predictors of a negative response to PD-1 blockade in MSI-H/dMMR gastrointestinal tumors. Clin Cancer Res 2021;27:3714–24.
10. Gibney GT, Weiner LM, Atkins MB. Predictive biomarkers for checkpoint inhibitor-based immunotherapy. Lancet Oncol 2016;17:e542–51.
11. Spranger S, Bao R, Gajewski TF. Melanoma-intrinsic β-catenin signalling prevents anti-tumour immunity. Nature 2015;523:231–5.

12. Kwon M, An M, Klempner SJ, Lee H, Kim K-M, Sa JK, et al. Determinants of response and intrinsic resistance to PD-1 blockade in microsatellite instability–high gastric cancer. Cancer Discov 2021;11:2168–85.

13. Kawazoe A, Kuboki Y, Shinozaki E, Hara H, Nishina T, Komatsu Y, et al. Multicenter phase I/II trial of napabucasin and pembrolizumab in patients with metastatic colorectal cancer (EPOC1503/SCOOP Trial). Clin Cancer Res 2020; 26:5887–94.

14. Bacher JW, Flanagan LA, Smalley RL, Nassif NA, Burgart LJ, Halberg RB, et al. Development of a fluorescent multiplex assay for detection of MSI-high tumors. Dis Markers 2004;20:237–50.

15. Hänzelmann S, Castelo R, Guinney J. GSVA: gene set variation analysis for microarray and RNA-seq data. BMC Bioinf 2013;14:7–7.

16. Subramanian A, Tamayo P, Mootha VK, Mukherjee S, Ebert BL, Gillette MA, et al. Gene set enrichment analysis: a knowledge-based approach for interpreting genome-wide expression profiles. Proc Natl Acad Sci U S A 2005;102:15545–50.

17. Guinney J, Dienstmann R, Wang X, de RA, Schlicker A, Soneson C, et al. The consensus molecular subtypes of colorectal cancer. Nat Med 2015;21:1350–6.

18. Wang G, Xu D, Zhang Z, Li X, Shi J, Sun J, et al. The pan-cancer landscape of crosstalk between epithelial–mesenchymal transition and immune evasion relevant to prognosis and immunotherapy response. NPJ Precis Oncol 2021; 5:56.

19. Zeng D, Li M, Zhou R, Zhang J, Sun H, Shi M, et al. Tumor microenvironment characterization in gastric cancer identifies prognostic and immunotherapeutically relevant gene signatures. Cancer Immunol Res 2019;7:737–50.

20. Conciatori F, Bazzichetto C, Falcone I, Pilotto S, Bria E, Cognetti F, et al. Role of mTOR signaling in tumor microenvironment: an overview. Int J Mol Sci 2018;19: 2453.

21. Ischenko I, D'Amico S, Rao M, Li J, Hayman MJ, Powers S, et al. KRAS drives immune evasion in a genetic model of pancreatic cancer. Nat Commun 2021;12: 1482.

22. Takeuchi Y, Tanegashima T, Sato E, Irie T, Sai A, Itahashi K, et al. Highly immunogenic cancer cells require activation of the WNT pathway for immunological escape. Sci Immunol 2021;6:eabc6424.

23. Derynck R, Turley SJ, Akhurst RJ. TGFβ biology in cancer progression and immunotherapy. Nat Rev Clin Oncol 2021;18:9–34.

24. Wu F, Cheng Y, Wu L, Zhang W, Zheng W, Wang Q, et al. Emerging landscapes of tumor immunity and metabolism. Frontiers Oncol 2020;10:575037.

25. Nizet V, Johnson RS. Interdependence of hypoxic and innate immune responses. Nat Rev Immunol 2009;9:609–17.

26. Ayers M, Lunceford J, Nebozhyn M, Murphy E, Loboda A, Kaufman DR, et al. IFN-γ–related mRNA profile predicts clinical response to PD-1 blockade. J Clin Invest 2017;127:2930–40.

27. Yamada K, Hori Y, Inoue S, Yamamoto Y, Iso K, Kamiyama H, et al. E7386, a selective inhibitor of the interaction between β-catenin and CBP, exerts antitumor activity in tumor models with activated canonical Wnt signaling. Cancer Res 2021;81:1052–62.

28. Zhang H, Bi Y, Wei Y, Liu J, Kuerban K, Ye L. Blocking Wnt/β-catenin signal amplifies anti-PD-1 therapeutic efficacy by inhibiting tumor growth, migration, and promoting immune infiltration in glioblastomas. Mol Cancer Ther 2021;20: 1305–15.

29. Hugo W, Zaretsky JM, Sun L, Song C, Moreno BH, Hu-Lieskovan S, et al. Genomic and transcriptomic features of response to anti–PD-1 therapy in metastatic melanoma. Cell 2016;165:35–44.

30. Chen P-L, Roh W, Reuben A, Cooper ZA, Spencer CN, Prieto PA, et al. Analysis of immune signatures in longitudinal tumor samples yields insight into biomarkers of response and mechanisms of resistance to immune checkpoint blockade. Cancer Discov 2016;6:827–37.

31. Apte RS, Chen DS, Ferrara N. VEGF in signaling and disease: beyond discovery and development. Cell 2019;176:1248–64.

32. Bourhis M, Palle J, Galy-Fauroux I, Terme M. Direct and indirect modulation of T cells by VEGF-A counteracted by anti-angiogenic treatment. Front Immunol 2021;12:616837.

33. Casak SJ, Donoghue M, Fashoyin-Aje L, Jiang X, Rodriguez L, Shen Y-L, et al. FDA approval summary: atezolizumab plus bevacizumab for the treatment of patients with advanced unresectable or metastatic hepatocellular carcinoma. Clin Cancer Res 2021;27:1836–41.

34. Motzer R, Choueiri TK. Lenvatinib plus pembrolizumab for renal cell carcinoma. New Engl J Med 2021;385:287.

35. Arora S, Balasubramaniam S, Zhang W, Zhang L, Sridhara R, Spillman D, et al. FDA approval summary: pembrolizumab plus lenvatinib for endometrial carcinoma, a collaborative international review under project Orbis. Clin Cancer Res 2020;26:5062–7.

36. Sveen A, Johannessen B, Tengs T, Danielsen SA, Eilertsen IA, Lind GE, et al. Multilevel genomics of colorectal cancers with microsatellite instability—clinical impact of JAK1 mutations and consensus molecular subtype 1. Genome Med 2017;9:46.

37. Soldevilla B, Carretero-Puche C, Gomez-Lopez G, Al-Shahrour F, Riesco MC, Gil-Calderon B, et al. The correlation between immune subtypes and consensus molecular subtypes in colorectal cancer identifies novel tumour microenvironment profiles, with prognostic and therapeutic implications. Eur J Cancer 2019; 123:118–29.

38. Dienstmann R, Vermeulen L, Guinney J, Kopetz S, Tejpar S, Tabernero J. Consensus molecular subtypes and the evolution of precision medicine in colorectal cancer. Nat Rev Cancer 2017;17:79–92.

39. Le DT, Durham JN, Smith KN, Wang H, Bartlett BR, Aulakh LK, et al. Mismatch repair deficiency predicts response of solid tumors to PD-1 blockade. Science 2017;357:409–13.

40. Uhlen M, Zhang C, Lee S, Sjöstedt E, Fagerberg L, Bidkhori G, et al. A pathology atlas of the human cancer transcriptome. Science 2017;357:eaan2507.

41. Marisa L, Blum Y, Taieb J, Ayadi M, Pilati C, Malicot KL, et al. Intratumor CMS heterogeneity impacts patient prognosis in localized colorectal cancer. Clin Cancer Res 2021;27:4768–80.